Power Law Statistics of Rippled Graphene Nanoflakes

Forrest H. Kaatz

Mesalands Community College, 911 South Tenth Street, Tucumcari, NM 88401

Electronic mail: fhkaatz@gmail.com

Adhemar Bultheel

Department of Computer Science, K.U.Leuven, Celestijnenlaan 200A, 3001 Heverlee, Belgium

Abstract

Graphene nanoflakes (GNFs) are predicted to possess novel magnetic, optical, and spintronic properties. They have recently been synthesized and a number of applications are being studied. Here we investigate the statistical properties of rippled GNFs (50 – 5000 atoms) at T=300K. An adjacency matrix is calculated from the coordinates and we find that the free energy, enthalpy, entropy, and atomic displacement all show power law behavior. The vibrational energy versus the Wiener index also shows power law character. We distinguish between using Euclidean topographical indices and compare them to topological ones. These properties are determined from atomic coordinates using MATLAB routines.

1. Introduction

Graphene [1] is a 2D allotrope of carbon (diamond, graphite, fullerene, carbon nanotubes, (CNTs)) that illustrates the amazing chemical and structural diversity of element number twelve. Recently, scientists have started considering limiting the size of the 2D sheet form of graphene, thus defining graphene nanoribbons, GNRs, and graphene nanoflakes, GNFs. One experimental method of attempting this is by using catalytic metal nanoparticles [2] cutting along crystallographic planes. When restricting the 2D sheet character of graphene by two dimensions in the plane, one creates GNFs, which theory predicts to have unique magnetic, optical, and spintronic properties.

GNFs may have a range of magnetic character, from ferromagnetic [3,4], to ferrimagnetic [5,6], to antiferromagnetic [7], depending on GNF geometry and topological frustration. These properties have enabled the design of spintronic NOR and NAND gates [7], which in principle can operate at room temperature. A spin-valve type effect [8] has been investigated in triangular GNFs. Additionally, hydrogenation can change the magnetic and electronic [9] character of the GNF. The optical properties of GNFs span the entire visible spectrum [10], opening the route to new nano optical devices. The electronic band structure as a function of increasing size [11] of triangular GNFs shows that semiconducting behavior exists for small GNFs.

An interesting question to consider when thinking about the thermal character of GNFs, is whether they are actually stable, or would they transform to another form of carbon, such as the fullerene or CNT shapes? This question has been modeled by density functional theory (DFT) and *ab initio* molecular dynamics (MD) calculations, with the result [12,13] that GNFs do not transform to a different allotrope, but neither are they

truly 2D, in the sense that the structure of the GNF becomes buckled and rippled at elevated temperatures. Annealing of the structures [12] found out-of-plane distortions as the temperature increased to 2400K, but no fundamental change in structure occurred.

Experimentally, the progress in creating GNFs is behind that of theoretical modeling. GNFs have been created using a 'top-down' approach from exfoliation of graphite [14], to chemical vapor deposition [15,16], to arc-discharged material [17]. Among the properties examined, electron field emission has predominated [14,16]. To date, a true nanoengineering 'bottoms-up' approach remains open to development. Thus, the truly exotic properties of GNFs, such as those already mentioned, remain to be explored.

2. Background

We employ a graph-theoretical approach, where nodes represent atoms, and an edge represents a bond between sites, *G = (V,E).* We create a graph of the GNF by creating bonds (links) between nearest neighbors up to 1.3 times the shortest neighbor distance from rippled MD models of graphene [18]. These vary from 50 to 5000 atoms and as created, are the asymmetric form [12] of a GNF. An adjacency matrix is created and may exist in two forms. The standard form is

$$A = \begin{cases} H(r_c - r_{ij}) & i \neq j \\ 0 & i = j \end{cases} \quad (1)$$

where the Heaviside step function $H(r_c - r_{ij}) = 1$ if $r_c < 1.3$*(shortest distance to r_{ij}), and i and j represent atomic sites, and r_c is the cutoff value. Alternatively, we may consider the actual Euclidean distances in the adjacency matrix [19,20], so that $H(r_c - r_{ij}) = e_{ij}$, the Euclidean distance between atoms.

The approach to modeling the free energy, enthalpy, and entropy has been discussed in the literature [21,22]. These can all be determined from the appropriate adjacency matrix. We also calculate one of the oldest indices, the Wiener index [23], as

$$W = \frac{1}{2}\sum_{i=1}^{n}\sum_{j=1}^{n} d_{ij} \tag{2}$$

where n is the number of atoms and d_{ij} is the shortest *path* distance between atoms i and j. In the standard form, the distances between atoms = 1, and in the Euclidean form [19], it is e_{ij}, so that we calculate W_E, the Euclidean 3D Wiener index. The collection of data starts from the atomic coordinates, and proceeds to calculating the adjacency matrix, and from it, all the results come from one MATLAB routine.

3. Results

In Fig.1, we show a plot of a rippled GNF with 500 atoms. In our modeling, the edge and corner atoms exist as shown in the figure, and as tabulated for the 50-5000 atom structures in Table 1. The coordination number of the GNF, N_C, ranges from 2.44 to 2.9404. The bond length varies around 1.42 Å. A histogram of the various bond lengths in the 500-5000 atom GNFs is shown in Fig.2, and the bond lengths range from 1.30 Å to 1.55 Å.

Once we have created the adjacency matrix, the statistical mechanics data can be calculated [21,22]. The partition function is:

$$Z(G,\beta) = \mathrm{Tr}(e^{\beta \mathbf{A}}) \tag{3}$$

where **A** is the adjacency matrix for the graph G, and $\beta = 1/(k_B T)$. At T=300K, we have β=38.68173/eV. The entropy can be determined as

$$S(G,\beta) = -k_B \sum_j \lambda_j p_j + k_B \ln(Z) \sum_j p_j \tag{4}$$

where λ_j is an eigenvalue of **A** and

$$p_j = \frac{e^{\beta\lambda_j}}{Z(G,\beta)} \tag{5}$$

is the probability that the ensemble occupies a microstate *j*. The free energy is the natural logarithm of the partition function,

$$F(G,\beta) = -\frac{\ln Z(G,\beta)}{\beta} \tag{6}$$

and the enthalpy can be defined as follows:

$$H(G,\beta) = -\frac{1}{Z(G,\beta)} \mathrm{Tr}(\mathbf{A}e^{\beta\mathbf{A}}). \tag{7}$$

We then plot the free energy, enthalpy, and entropy, per bond, versus the number of bonds in the GNF. This results in plots with good power law regression statistics as shown in Fig. 3. The distinction between Fig. 3(a) and (b) is that in (a), we have used an adjacency matrix with Euclidean distances, and in (b), we have used the standard adjacency matrix with zeros and ones. The best-fit equations in (a) have different leading coefficients, so that the entropy and enthalpy coincide (neglecting the sign difference) for small (< 50 atoms) GNFs, and since the slope is different, the plots diverge for larger GNFs. Since we use a value of the Boltzmann constant in terms of eV, the units on our thermodynamic calculations are: entropy (eV/K), enthalpy (eV), and free energy (eV). These quantities are divided by the number of bonds in the GNF and plotted versus N_B, to give a power law plot. The asymptote of zero for large N_B makes intuitive sense, since if we imagine the data/bond is finite, then as the number of bonds becomes large, we have

zero as a limit. Note that the free energy and enthalpy have their signs reversed to allow them to be plotted.

We now proceed to calculate some related parameters of interest. In the harmonic approximation [24], the frequency of the stretching vibration of a carbon-carbon bond is given by:

$$\nu = \frac{1}{2\pi}\sqrt{\frac{k}{\mu}} \tag{8}$$

where k is the force constant (about 305 N/m for graphene [25]) between nearest neighbor carbon atoms and μ is the reduced mass. The total intramolecular energy, E_{int} can be divided into two parts; a variable term U_{var} and a constant term U_{con}. We conclude that the variable term can be written [24] as:

$$U \cong \sum \frac{1}{\sqrt{M_1 M_2 / M}} \tag{9}$$

where the proportionality constant depends on the force constant, but not the mass dependence. If we rewrite this in terms of our GNF, we have:

$$U = \sum \sqrt{\frac{n}{Cn_1 n_2}} \tag{10}$$

where $n = n_1 + n_2$, and n_1 and n_2 are the number of carbon atoms on the two sides of the vibrating bond. We may compare this to the relationship [23,24] for the Wiener index:

$$W = \sum n_1 n_2 . \tag{11}$$

Now in order to linearize U, we note that the minimum and maximum values of the product n_1n_2 are (n - 1) and $(n/2)^2$, respectively. The middle value is

$$\xi = \frac{n^2}{8} + \frac{n-1}{2} \tag{12}$$

and we expand U as a power function about $x = \xi$

$$(Cx)^{-1/2} \approx f(\xi) + f'(\xi)(x - \xi) \tag{13}$$

where

$$f(\xi) = \frac{1}{\sqrt{C}} \sqrt{\frac{8n}{n^2 + 4n - 4}}. \tag{14}$$

If we write C = 12 amu, then to a first approximation we have

$$U \approx \frac{1}{\sqrt{12}} N_B \sqrt{\frac{8n}{n^2 + 4n - 4}} \tag{15}$$

Since *n* is the number of atoms in the GNF and we calculate N_B through each iteration of the MATLAB program, we can determine the approximate values for U. Now both U and W have power law character, so we plot U versus W and W_E in Figure 4. These results show good regression features. The only distinction is that W_E has slightly larger values, but behaves in the same manner as W. The MATLAB code for W has been examined previously [26], but we have adapted it to work with an adjacency matrix.

In the harmonic approximation, we may also consider the vibrational excitation energy from the static position of the GNF. Previous calculations [27], show that the summed displacement may be calculated as:

$$\langle X_i X_i \rangle = \sqrt{\sum_{i=1}^{n} (\Delta x_i)^2} = \sqrt{\frac{W}{nk\beta}} \tag{16}$$

where β = 38.68173/eV, *k* is the force constant between carbon atoms (305 N/m), *n* is the number of atoms, and W is the Wiener index. In Fig. 5, we show the dependence of N_B, U, W, and <XX> on the number of carbon atoms N. The values of the summed

displacement range from 0.3047Å to 7.4107Å for 50 to 5000 atoms, respectively. If we were to consider the average displacement per bond, the values would be 0.002498Å and 0.0005041Å, for 50 and 5000 atoms, respectively. The data all show good regression features.

4. Conclusions

We have determined the power law behavior of the free energy, enthalpy, entropy, and atomic displacement of GNFs consisting of 50-5000 atoms at T=300K. The vibrational energy versus the Wiener index also shows power law character. There are some minor distinctions when using the Euclidean Wiener index, which we have included for completeness.

Acknowledgements

F.H. Kaatz thanks A. Fasolino for sharing atomic coordinates of rippled graphene, and thanks E. Estrada and A. Vodopivec for discussing concepts related to the manuscript.

Tables and Captions

Table 1

N	N_1	N_2	N_3	N_C	Ave Bond Å
50	5	18	27	2.44	1.4248
100	7	26	67	2.60	1.4219
500	16	62	422	2.812	1.4228
1000	22	86	892	2.87	1.4229
2500	35	138	2327	2.9168	1.4239
5000	50	198	4752	2.9404	1.4238

Table 1 Caption

N is the number of atoms in the GNF, N_1, N_2, and N_3, are the number of one, two, and three fold coordinated atoms in the GNF, and N_C is the coordination number. The average bond length is in Angstroms.

Figure Captions

Figure 1

MATLAB plot of a 3D rippled GNF with 500 atoms.

Figure 2

Histogram of the bond lengths (in Angstroms) of the 500-5000 GNFs.

Figure 3

(a) Plots of the free energy, enthalpy, and entropy / bond versus the number of bonds. The data clearly exhibits power law character. This plot uses a Euclidean adjacency matrix.
(b) Plots of the free energy, enthalpy, and entropy / bond versus the number of bonds. The data clearly exhibits power law character. This plot uses a standard adjacency matrix.

Figure 4

Vibrational energy, U, versus the standard Wiener index, W, and the 3D Euclidean Wiener index W_E. The data follows a power law.

Figure 5

Power law plots of N_B, U, W, and <XX> versus the number of carbon atoms, N. The statistics and regression of the data are quite good.

Figure 1

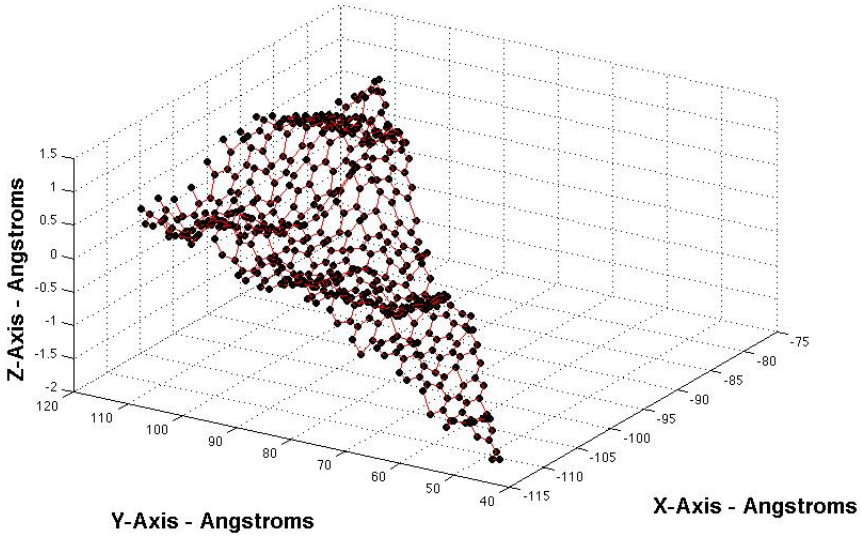

Figure 2

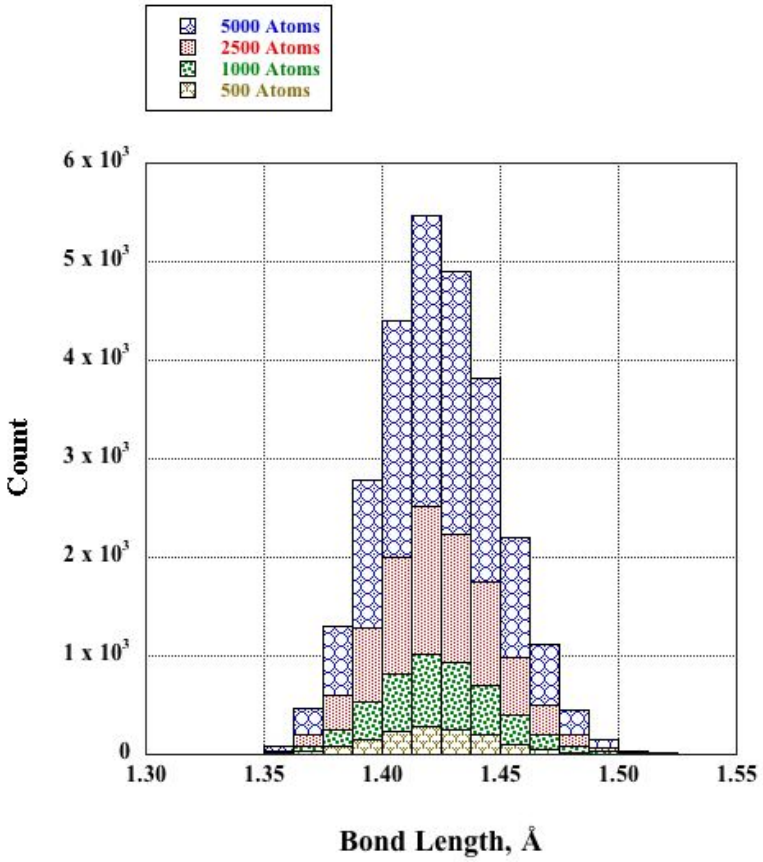

Figure 3(a)

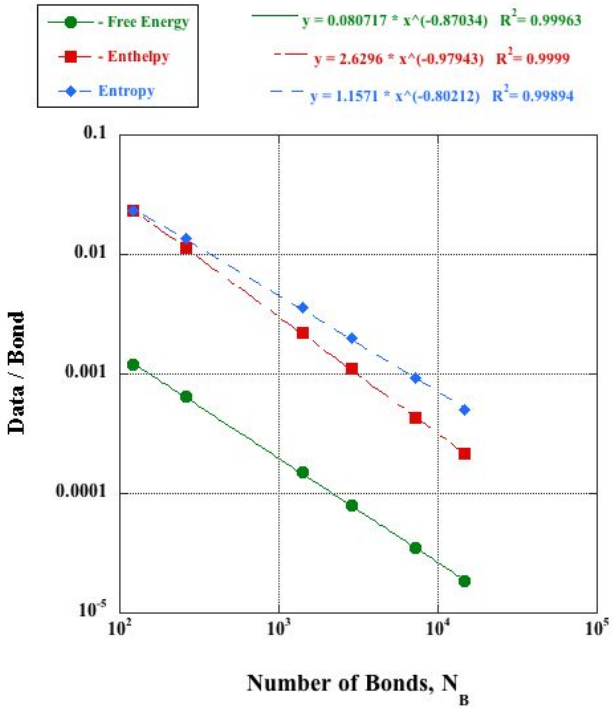

Figure 3(b)

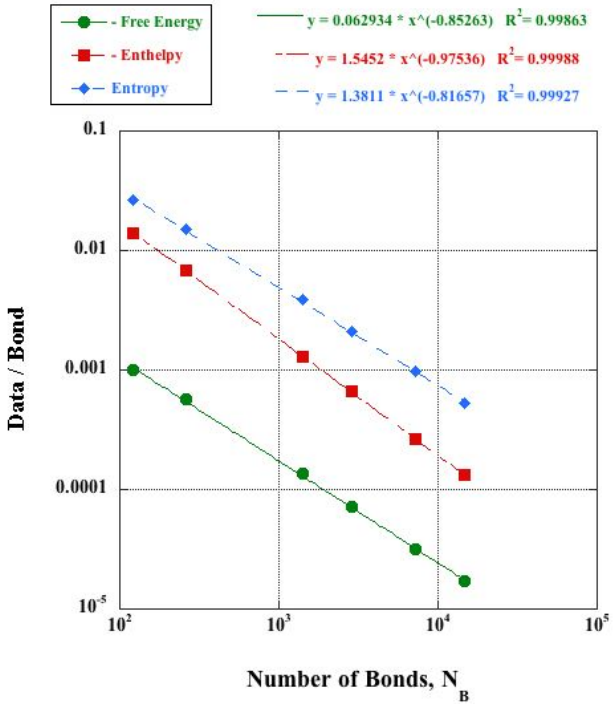

Figure 4

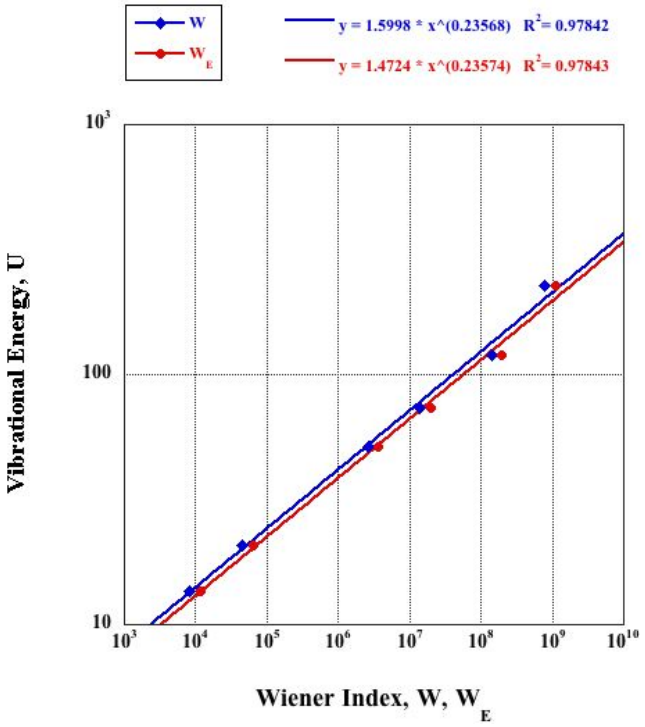

Figure 5

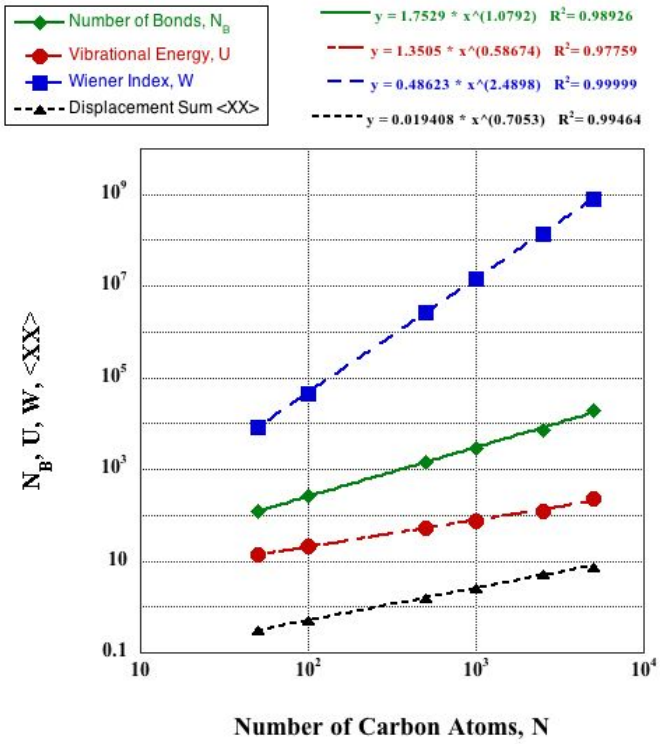

References

[1] V. Singh, D. Joung, L. Zhai, S. Das, S.I. Khondaker, and S. Seal, Prog. Mater. Sci. 56, (2011) 1178.
[2] L. C. Campos, V. R. Manfrinato, J. D. Sanchez-Yamagishi, J. Kong, and P. Jarillo-Herrero, Nano Lett. 9(7), (2009) 2600.
[3] J. Zhou, Q. Wang, Q. Sun, and P. Jena, Phys. Rev. B 84, (2011) 081402.
[4] X. Li and Q. Wang, Phys. Chem. Chem. Phys. 14, (2012), 2065.
[5] W.L. Wang, S. Meng, and E. Kaxiras, Nano Lett. 8, (2008) 241.
[6] W. Sheng, Z. Y. Ning, Z. Q. Yang, and H. Guo, Nanotechnology 21, (2010) 385201.
[7] W.L. Wang, O.V. Yazyev, S. Meng, and E. Kaxiras, Phys. Rev. Lett. (2009) 157201.
[8] H. Sahin, R. T. Senger, and S. Ciraci, J. Appl. Phys. 108, (2010) 074301.
[9] Y. Zhou, Z. Wang, P. Yang, X. Sun, X. Zu, and F. Gao, J. Phys. Chem. C 116, (2012), 5531.
[10] A.M Silva, M.S. Pires, V.N. Freire, E.L. Albuquerque, D.L. Azevedo, and E.W.S. Caetano J. Phys. Chem. 114, (2010) 17472.
[11] H. Shi, A.S. Barnard, and I.K. Snook, Nanotechnology 23, (2012) 065707.
[12] A.S. Barnard and I.K. Snook, J. Chem. Phys. 128, (2008) 094707.
[13] A. Kuc, T. Heine, and G. Seifert, Phys. Rev. B 81, (2010) 085430.
[14] S. Vadukumpully, J. Paul, and S. Valiyaveettil, Carbon 47, (2009) 3288.
[15] N. G. Shang, P. Papakonstantinou, M. McMullan, M. Chu, A. Stamboulis, A. Potenza, S. S. Dhesi, and H. Marchetto, Adv. Funct. Mater. 18, (2008) 3506.
[16] N. Soin, S.S. Roy, S. Roy, K.S. Hazra, D.S. Misra, T.H. Lim, C.J. Hetherington, and J. A. McLaughlin, J. Phys. Chem. 115, (2011) 5366.
[17] C.G. Salzmann, V. Nicolosi, and M.L.H. Green, J. Mater. Chem. 20, (2010) 314.
[18] A. Fasolino, J.H. Los, and M.I. Katsnelson, Nature Mater. 6, (2007) 858.
[19] S. Nikolic, N. Trinajstic, Z. Mihalic, and S. Carter, Chem. Phys. Lett. 179, (1991) 21.
[20] A. Vodopivec, F.H. Kaatz, and B. Mohar, J. Math. Chem. 47, (2010) 1145.
[21] E. Estrada, and N. Hatano, Chem. Phys. Lett. 439, (2007) 247.
[22] F.H. Kaatz, E. Estrada, A. Bultheel, and N. Sharrock, Physica A 391 (2012), 2957.
[23] H. Wiener, J. Am. Chem. Soc. 69, (1947) 17.
[24] I. Gutman and I.G. Zenkevich, Z. Naturforsch. A 57, (2002) 824.
[25] S.Y. Davydov, Phys. of the Solid State 52, (2010), 1947.
[26] A.R. Ashrafi and M.R. Ahmadi, Internet J. of Nanotechnology 1,2 (2005).
[27] E. Estrada and N. Hatano. Chem. Phys. Lett. 486, (2010) 166.